The FASEB Journal express article10.1096/fj.02-1201fje. Published online July 18, 2003.

Lowering of tumor interstitial fluid pressure specifically augments efficacy of chemotherapy

Alexei V. Salnikov,* Vegard V. Iversen,[†] Markus Koisti,[‡] Christian Sundberg,* Lars Johansson,[‡] Linda B. Stuhr,[†] Mats Sjöquist,[§] Håkan Ahlström,[‡] Rolf K. Reed,[†] and Kristofer Rubin*

*Department of Medical Biochemistry and Microbiology, Uppsala University, BMC, Box 582 SE-751 23 Uppsala, Sweden; [†]Department of Physiology, University of Bergen, N-5009 Bergen, Norway; [‡]Department of Radiology, University Hospital, SE-751 85 Uppsala, Sweden; [§]Department of Medical Cell Biology, Section of Physiology, Uppsala University, BMC, Box 571 SE-751 23 Uppsala, Sweden

Corresponding author: Kristofer Rubin, Dept. of Medical Biochemistry and Microbiology, Uppsala University, BMC, Box 582 SE-751 23 Uppsala, Sweden. E-mail: Kristofer.Rubin@imbim.uu.se

ABSTRACT

Chemotherapy of solid tumors is presently largely ineffective at dosage levels that are compatible with survival of the patient. Here, it is argued that a condition of raised interstitial fluid pressure (IFP) that can be observed in many tumors is a major factor in preventing optimal access of systemically administered chemotherapeutic agents. Using prostaglandin E_1-methyl ester (PGE_1), which is known transiently to reduce IFP, it was shown that 5-fluorouracil (5-FU) caused significant growth inhibition on two experimental tumors in rats but only after administration of PGE_1. Furthermore, timing experiments showed that only in the period in which IFP is reduced did 5-FU have an antitumor effect. These experiments uniquely demonstrate a clear and, according to the starting hypothesis, logical, synergistic effect of PGE_1 and 5-FU that offers hope for better treatment of many tumors in which raised IFP is likely to be inhibiting optimal results with water-soluble cancer chemotherapeutic agents.

Key words: 5-fluorouracil • prostaglandin E • histopathology • apoptosis • vasculature

Chemotherapy against solid malignancies is often ineffective. This can partly be explained by the development of multidrug resistance to anticancer drugs by the carcinoma cells (1). Another reason, which is attracting increased attention, is the inefficient transport of anticancer drugs into tumor tissue (2–4). The impaired transport of anticancer drugs into the tumor interstitium has been attributed to contorted tumor vasculature, changes in the extracellular matrix (ECM), and to pathologically increased tumor interstitial fluid pressure (TIFP) (2, 5–7). Both human and experimental solid malignancies are characterized by an elevated TIFP (8–11). The pathophysiological processes leading to elevated TIFP are poorly understood. Altered vascular structure, high vascular permeability to plasma proteins, and impaired lymphatic drainage have been suggested to be important for the generation of high TIFP (6, 11, 12). TIFP is reduced in experimental tumors that have been treated with taxane, suggesting that malignant cell proliferation increases TIFP (13).

Lowering of TIFP in experimental carcinomas by prostaglandin E_1-methyl ester (PGE_1) increases capillary-to-interstitium transport of ^{51}Cr-EDTA (14). Infusion of the bradykinin agonist Cereport in rats bearing experimental tumors reduces TIFP, decreases blood flow to the tumor, increases pore size of the vasculature and vessel surface area within the tumor, and increases deposition of [^{14}C]carboplatin in the tumor tissue (15). Furthermore, treatment for 4 days with the selective platelet-derived growth factor (PDGF) receptor inhibitor STI571 (Glivec) or with a specific inhibitor of PDGF-B lowers TIFP and increases uptake and sensitivity to 5-fluorouracil (5-FU) and Taxol in experimental carcinoma (16, 17).

Results from clinical trials and animal experiments show that treatment with the tyrosine kinase inhibitor ZD 1839 (Iressa) (18, 19), a COX-2 inhibitor (Celecoxib) (20), and the selective endothelin A receptor antagonist ABT-627 (Atrasentan) (21) improves efficacy of conventional chemotherapy for solid tumors. It might be that additative effects of these inhibitors are due in part to lowering of TIFP.

A direct correlation between TIFP and efficacy of chemotherapy has not been established. In the present study, we have devised an experimental system to investigate this relationship. We used PGE_1 to transiently lower TIFP in experimental carcinomas and combined this treatment with 5-FU, which has a reported half-life of ~10–20 min in rats (22). By administering 5-FU at times when TIFP was lowered by PGE_1, or alternatively, outside of this time period, we could directly assess whether TIFP generates a functional barrier to chemotherapy with this cytostatic.

MATERIAL AND METHODS

Animals and tumors

The PROb subclone of the rat colonic carcinoma cell line DHD-K12 (23) was transplanted s.c. to BD-IX rats (Harlan, Oxon, England). Mammary carcinomas were induced in Wistar-Möller rats (Möllergaard, Lille Skensved, Denmark) by dimethyl-benz-anthracene (DMBA) as previously described (14). Animals were anesthetized during all manipulations with i.p. administration of Inactin (120 mg/kg body weight, sodium 5 *s*-butyl-5-ethyl-2-thiobarbiturate; Research Biochemicals International, Natick, MA) or by inhalation of isoflurane. Animal experiments were approved by the Ethical Committee for Animal Experiments in Uppsala (Sweden) and, where appropriate, by the Norwegian Committee for Animal Research.

Treatment

5-FU was given i.p. every third day at a dose of 1.5 mg/kg for DMBA and 1 mg/kg for PROb tumor-bearing rats. These doses were determined to be minimal for the detection of antitumor effects in the respective tumor models with the treatment regimes used (16) (data not shown). Prostaglandin E_1-methyl ester (15 µg; P439; Sigma, St. Louis, MO) in 1 ml phosphate buffered saline (PBS) with 2.5% ethanol was injected s.c. around the tumor. Animals with DMBA-induced tumors receiving PGE_1 were randomized to one of five groups receiving 5-FU at a) 30 min before PGE_1 (n=8), b) 15 min before PGE_1 (n=8), c) 1 min after PGE_1 (n=7), d) 15 min after PGE_1 (n=10), and e) 30 min after PGE_1 instillment (n=8). Animals with PROb tumors receiving PGE_1 were randomized to one of three groups receiving 5-FU at a) 15 min before PGE_1 (n=6), b) 1 min after PGE_1 (n=11), and c) 15 min after PGE_1 instillment (n=6). Control animals received

PGE_1 and PBS or PBS containing 2.5% ethanol and 5-FU. Experiments were terminated on day 11 in the DMBA groups and on day 15 in the PROb groups. Average sizes of PROb- and DMBA-induced tumors at the start of the treatment was 2.2 ± 1.1 cm^3 (±SD, n=80), and 1.8 ± 1.4 cm^3 (n=61), respectively.

Measurement of tumor growth

Tumor size was measured externally before treatment. PROb tumor volumes were calculated assuming a cubic form of the tumor, because that form was found to correspond most closely to the recorded end point tumor weights. DMBA-induced tumor volumes were calculated assuming a cylindrical form of the tumor according to the formula: $V=(a^2*b)\pi/6$, where a is the shortest transversal diameter and b is the longest transversal diameter. The location of the DMBA-induced tumors excluded external measurements in more than two dimensions.

Microdialysis technique

Microdialysis was performed as previously described (14). Capillary-to-interstitium transport of 5-FU was assessed by microdialysis after i.v. injection of 37 MBq 5-fluoro[6-^{3}H]uracil ([^{3}H]5-FU) (Nycomed Amersham, Buckinghamshire, UK). Area under the curve (AUC) for plasma and for the tumor was calculated as the product of radioactivity (cpm) and time, respectively. Transport was expressed as AUC tumor/AUC plasma.

Maganetic resonance (MR) Imaging

NC100150 Injection (24), a particulate, iron oxide-based intravascular contrast agent has previously been used for assessment of the blood volume in tumors (25) and other tissues (26), using quantitative measurements of the longitudinal relaxation time T1. Rats were imaged in a 1.5T clinical MR scanner (Gyroscan Intera, Philips Medical Systems, Best, The Netherlands). The contrast agent was injected at a dose of 2 mg Fe/kg body weight 5 min after instillment of either PBS (control group, n=5) or PGE_1 (treatment group, n=7). MR imaging, using an inversion recovery sequence with multiple readouts, which lasted for 4 min, was performed at baseline and at 2 min after injection of the contrast agent. The delay of 2 min was used in order to allow filling of the vascular space. T1 was assessed by fitting a monoexponential curve describing the longitudinal relaxation time, T1, to the images following the inversion prepulse on a pixel by pixel basis. The relative increase in R1 (1/T1), which reflects the blood volume (26), was calculated for all the image pixels yielding a parametric R1 map, and the increase in R1 was compared between the viable parts of the tumors in the two groups using a t test.

Transcapillary extravasation of iodine-labeled albumin

PGE_1 or PBS was injected around s.c. PROb tumors in anesthetized rats, and immediately thereafter, 0.4 MBq of human serum albumin (HSA) labeled with ^{125}I (Isopharma, Kjeller, Norway) was injected i.v. Twenty-five minutes after injection of ^{125}I-HSA, ^{131}I-HSA (Isopharma) was injected i.v., and blood samples were obtained by cardiac puncture. Thereafter, the animals were killed and radioactivity of the whole tumor was determined in a Wallac γ-counter (Turku, Finland) with automatic background and spillover correction. Transcapillary albumin extravasation was determined as the 25-min distribution volume of ^{125}I-HSA, that is, as

counts per minute ^{125}I in the tumor divided by ^{125}I counts per minute per ml plasma. The distribution volume was expressed per gram wet weight.

Determination of PROb tumor blood flow, using radioactive isotope-labeled microspheres

Anesthetized rats (Inactin) were subjected to tracheotomy, and a polyethylene catheter was inserted into the right carotid artery and placed with its tip at the aortic root just above the aortic valves. The right femoral artery was cannulated for continuous recording of the blood pressure and to a syringe pump withdrawing blood at a rate of 0.5 ml/min (flow reference), when activated. This flow reference acts as an "artificial organ" with a known blood flow. The absolute blood flow to any organ can then be calculated by comparing the amount of microspheres trapped in an organ to that trapped in the reference catheter. The syringe pump, acting as a flow reference, was activated 30 min after surgical procedures. A 0.15 ml suspension of ^{141}Ce- or ^{113}Sn-labeled microspheres (15 μm diameter, New England Nuclear, Boston, MA) was injected as soon as the flow to the syringe pump had stabilized (~5 s). About 10 s after the injection, the pump was stopped and the blood sample was transferred to a vial for radioactive content determination (Nuclear-Chicago, Chicago, IL). The tissue surrounding the tumor was then instilled with 1 ml of PBS containing 2.5% ethanol or PGE_1. This was allowed to act for 15 min, and then a second blood flow determination was performed as described above. Tissue samples of kidney, heart, lung, liver, diaphragm, lymph node, and the tumor was dissected out, weighed, and analyzed for radioactive content. The radioactive content of ^{141}Ce and ^{113}Sn was determined at their main energy peaks. The crossover from ^{141}Ce to the ^{113}Sn window was determined from a pure sample. Blood flow was then calculated as $(CPM_{tissue}/CPM_{reference}) \times Flow_{reference}$ and related to its wet weight.

Reduction of blood pressure

To lower blood pressure in PROb carcinoma-bearing rats, the vasodilating agent sodium nitroprusside (Nipride, Roche, Basel, Switzerland) was used. Nipride was dissolved in saline with 5% glucose at a dose of 60 μg/ml and administered by continuous i.v. infusion at a rate of 1–2.5 ml per hour. Systemic arterial blood pressure was measured in the right femoral artery, and TIFP was measured by the "wick-in-the needle" technique (n=5), both as previously described (14).

Antibodies

Anti-rat CD31/PECAM-1 antibody detecting endothelial cells, anti-ED1 antigen antibody detecting macrophages, and anti-granulocyte antibody were from Serotec (Oxford, UK). Anti-CD5 antibody detecting T-lymphocytes, anti-CD45RA antibody detecting B-lymphocytes, and anti-RT1B antibody detecting MHC class II antigen were from BD PharMingen (San Diego, CA). Anti-NG2 antibody detecting pericytes was from Chemicon (Temecula, CA). An anti-α smooth muscle actin antibody and an anti-pan cytokeratin antibody were from Sigma.

Immunohistochemistry and histochemistry

Immunohistochemistry on 6 μm cryosections was performed as previously described (27) at the end point of experiments. Apoptosis was detected by TUNEL staining (TACS TdT in situ

apoptosis detection kit; R&D Systems, Abingdon, Oxon, UK) performed according to the manufacturer's recommendations, with the modifications that the signal was enhanced by Vectastain ABC elite kit (Vector, Burlingame, CA) and color was developed with a DAB kit (Vector). To analyze tumor morphology, we stained sections with hematoxylin-eosin or, to highlight ECM rich in collagen, with Accustain Trichrome Stains (Masson; Sigma, St. Louis, MO) following the manufacturer's recommendations. Images were analyzed using a Nikon Labophot microscope and captured with a SPOT Insight digital camera (Diagnostic Instruments, Sterling Heights, MI), using the SPOT 3.4 software.

Stereometric analysis of tumor vessels

Tumor vessel parameters were assessed by stereologic quantification of CD31-positive structures as previously described (28, 29).

Statistical methods

Data were analyzed using the unpaired, two-tailed Student's *t* test. One-way ANOVA was used to test differences between several groups and when appropriate was followed by post hoc Boneferroni and Newman-Keul tests. $P<0.05$ was considered statistically significant.

RESULTS

Effects of PGE_1 on tumor blood flow, blood volume, and protein extravasation

Instillment of PGE_1 around PROb tumors transiently lowers TIFP and increases total tissue water and capillary-to-interstitium transport of ^{51}Cr-EDTA in the tumors (14). To investigate potential physiological explanations for these phenomena, we studied the effects of PGE_1 on blood volume, blood flow, and protein extravasation in PROb tumors. Blood volume, as determined by MR imaging, was not changed in tumors treated with PGE_1 (n=7) compared with controls (n=5; $P>0.05$) (Fig. 1A). Furthermore, no discernable differences in distribution patterns of the contrast agent were observed between tumors treated with PGE_1 or controls (Fig. 1B). Blood flow, determined by radiolabeled 15-μm microspheres, increased after PGE_1 or PBS instillment in all organs studied during the 15 min study period, and it was unrelated to treatment. There was no significant difference in tumor blood flow after instillment of PGE_1 compared with PBS instillment (Fig. 1C). Extravasation of ^{125}I-HSA was similar in tumor treated with PGE_1 (n=5) and saline vehicle (n=5), that is, 0.027 ± 0.012 ^{125}I-HSA ml/g and 0.024 ± 0.015 ml/g, ($P>0.05$) (Fig. 1D). The latter finding indicates that treatment with PGE_1 did not increase plasma protein leakage from blood to tumor interstitium. To investigate whether TIFP is affected by changes of blood pressure, we used the vasodilating agent sodium nitroprusside. Continuous lowering of blood pressure by 20–25% for a time period of 1 h with sodium nitroprusside did not affect the TIFP in PROb carcinomas (Fig. 1E).

Effect of PGE_1 on capillary-to-interstitium transport of 5-FU

The effect of PGE_1 on capillary-to-interstitium transport of 5-FU in PROb tumors was investigated using microdialysis. Capillary-to-interstitium transport of [^{3}H]5-FU was significantly increased after local instillment of PGE_1 compared with PBS (Fig. 2A). Qualitatively similar results were obtained in DMBA-induced tumors (data not shown).

Effects of PGE_1 on antitumor activity of 5-FU in PROb and DMBA-induced tumors

Rats carrying PROb- and DMBA-induced tumors were treated every third day with combinations of PGE_1, 5-FU, and PBS, and tumor sizes were recorded. 5-FU was administered i.p. at various time points before and after the instillment of PGE_1. Maximal radioactivity in plasma following i.p. injection of [^{3}H]5-FU was observed after 15 min (Fig. 2B). The cytostatic was given at low doses that lacked any significant effect on growth in PROb and DMBA tumors. The rate of PROb tumor growth was significantly retarded when 5-FU was administered 1 min after instillment of PGE_1, compared with tumors in animals receiving either PBS and 5-FU or PGE_1 and PBS (Fig. 2C). The increase of PROb tumor growth during a 10-day time period was significantly retarded when 5-FU was administered 1 min after instillment of PGE_1 (26 ± 6%; ±SE; n=11; P<0.01) compared with tumors from animals receiving either PBS and 5-FU (80 ± 11%; n=34) or PGE_1 and PBS (95 ± 13%; n=10) (Fig. 2D). Similarly, DMBA-induced tumors were significantly retarded in growth (14 ± 25%; n=7; P<0.05) when 5-FU was administered 1 min after the instillment of PGE_1 compared with size increases for tumors treated with PBS and 5-FU (71 ± 13%; n=12) or with PGE_1 and PBS (114 ± 43%; n=6).

In both PROb- (Fig. 2D) and DMBA-induced tumors (Fig. 2E), a marked dependence on the time point for 5-FU administration relative to the PGE_1 instillment was evident during the 10-day treatment period. Thus, if administered 30 min before the instillment of PGE_1, 5-FU had no effect on growth of DMBA-induced tumors (158 ± 24%; n=8). Likewise, 5-FU did not have any significant effect when administered 30 min after PGE_1 in DMBA tumors (104 ± 25%; n=8) (Fig. 2E). Administration of 5-FU 30 min before instillment of PGE_1 combined with a second instillment of PGE_1 12 h later (n=13) did not influence growth rate of PROb tumors (data not shown). In DMBA-induced tumors, when 5-FU was injected 15 min before or 15 min after the PGE_1 instillment, tumor growth was significantly inhibited (Fig. 2E) (P<0.03). PROb tumor growth was significantly retarded when 5-FU was administered 15 min after PGE_1 (Fig. 2D). Treatment with PGE_1 and PBS or with 5-FU and PBS had no significant effects on tumor growth when compared with tumors that had been treated with PBS only (data not shown).

Effects of combination treatment with PGE_1 and 5-FU on PROb tumor morphology

PROb tumors displayed a peripheral zone with viable tissue containing carcinoma cells organized in abnormal glandular structures and also stromal cells. A second, central zone was mostly acellular, containing ECM components and cell debris. In PROb tumors treated with 5-FU administered 1 min after a PGE_1 instillment, the viable zone was on average 41 ± 9% of total tumor area (n=8). The corresponding figure for tumors from the control groups was 49 ± 6% (n=17; P>0.05). Cell density, quantified by counting cells in hematoxylin-stained sections, was similar in tumors derived from animals subjected to the different treatment regimes (Fig. 3A). The cellular density in tumors from animals treated with 5-FU injected 1 min after instillment of

PGE_1 was, however, significantly lower, although this difference was small. The density of carcinoma cells, identified by cytokeratin expression, was significantly lower in tumors treated with 5-FU administered 1 min after PGE_1 instillment (cytokeratin positive area, 25 ± 2%; ±SD, n=3, P<0.05), compared with tumors from any of the other groups, including those treated with 5-FU 15 min before the instillment of PGE_1 (70 ± 10%; n=3) (Fig. 3B, Fig. 4). Carcinoma cells, identified by morphology, which did not stain for cytokeratin, localized predominantly in the area juxtapositioned to the apoptotic zone at the interphase between the viable and necrotic zones (data not shown).

Effects of combination treatment with PGE_1 and 5-FU on apoptosis in PROb tumors

In PROb tumors from animals that had been subjected to various treatment regimes for 15 days, several small regions with an increased density of apoptotic cells toward the central zone were present. Furthermore, a well-defined apoptotic front at the interphase between the viable and necrotic zones were observed. The apoptotic index in tumors from animals treated with 5-FU 1 min after PGE_1 instillment was significantly higher (2.9 ± 0.3; n=4; P<0.05) compared with control tumors from animals treated with PBS and 5-FU (1.9 ± 0.5; n=4) or with PGE_1 and PBS (1.5 ± 0.08; n=4) (Fig. 3C). The apoptotic index in tumors from animals treated with 5-FU 15 min before the instillment of PGE_1 was not significantly different from controls (1.7 ± 0.28; n=4) (Fig. 3C).

Effects of combination treatment with PGE_1 and 5-FU on vessel density in PROb tumors

Endothelial cells were visualized by staining with an anti-CD31/PECAM-1 antibody (Fig. 4). The density of CD31-positive structures in the viable zone was significantly decreased in the PROb tumor groups that had received 5-FU compared with the group that had been treated with PGE_1 and PBS (Table 1). Stereometric analyses revealed that the mean section area of vessels and mean diameter of vessels were significantly larger in PROb tumors treated with 5-FU 1 min after the instillment of PGE_1 compared with the groups treated with 5-FU according to the other regimes.

Vessel coverage by pericytes (NG2 staining) and smooth muscle cells (α-smooth muscle actin staining) were qualitatively similar in tumors subjected to the various treatment regimes (data not shown).

Effects of combination treatment with PGE_1 and 5-FU on leukocyte infiltration in PROb tumors

MHC class II antigen and B-lymphocytes were not detected in tumors from any of the treatment groups (data not shown). Only limited numbers of T-lymphocytes and granulocytes were observed (Fig. 5). In contrast, macrophages were abundant, amounting to ~14% of the total cell number in the viable zone. Macrophages were also present in the central necrotic zone. The number of macrophages, T-lymphocytes, and granulocytes per tumor unit area did not differ significantly between tumors in animals subjected to the various treatment regimes.

DISCUSSION

We show that reducing TIFP in experimental carcinomas increases the delivery of the low molecular weight cytostatic 5-FU into the tumors and improves treatment efficacy. Local administration of PGE_1 transiently lowers TIFP in both PROb- and DMBA-induced experimental carcinomas (14). The TIFP reaches a minimum after 10–15 min and returns to the initial TIFP value within 60 min after treatment with PGE_1 (14). 5-FU has a $t_{1/2}$ of ~10–20 min (22) and a rapid uptake into the circulation after i.p. injection. By combining treatment with PGE_1 and 5-FU, we could directly test the hypothesis that tumors are most sensitive to 5-FU while TIFP is low. The time profile for potentiation of 5-FU efficacy closely resembled that by which TIFP was reduced by PGE_1, when taking into account the time required for 5-FU to reach maximal plasma concentration after an i.p. injection. Our data strongly suggest that the pathologically high TIFP, which is a hallmark of solid tumors (8–11), does form a barrier to drug delivery.

Uptake of 5-FU into tumors would be favored by mechanisms related to increased blood flow and/or surface area of the capillary wall due to the PGE_1 injection. Increased blood flow and surface area of the capillary wall will bring the tumor interstitium in closer contact with the rapidly falling plasma concentration of 5-FU. The present data showing that blood flow and blood volume in tumors were unaltered by the PGE_1 treatment indicate that mechanisms other than increased blood flow are responsible for the lowering of TIFP and the increased efficacy of 5-FU. This notion is further strengthened by the qualititatively similar distribution patterns of the high molecular weight MR contrast agent, and similar degree of albumin extravasation in tumors treated with PGE_1 and in controls, showing that neither blood flow nor vessel integrity were affected by the PGE_1 treatment.

The increased mean section area and diameter of vessels reported here indicate that vessel surface area was extended in tumors in animals treated with 5-FU 1 min after PGE_1 instillment. The flux of low molecular weight substances through the capillary wall depends, in part, on vessel morphology such as the length, diameter, and geometric arrangement. The extension of the vessel surface area, therefore, may promote the increased 5-FU transport into the tumor interstitium. Similar observations are described for modulation of [^{14}C]carboplatin deposition in tumor interstitium by the bradykinin agonist, Cereport (30). Alternatively, the extension of the vessel surface area may be due to increased apoptosis, because it has been reported that increased apoptosis leads to a decompression of the blood vessels in solid tumors (13). The present results showing that only the effective combination of PGE_1 and 5-FU resulted in an increased vessel surface area suggest that vessel dilation is a consequence of, and not the reason for, the increased efficacy of 5-FU when administered during lowered TIFP.

The mechanisms by which PGE_1 lowers TIFP are not fully understood. In a previous report, we showed that instillment of PGE_1 around tumors transiently lowers mean arterial blood pressure (14). The decrease in blood pressure is, however, not likely to be involved in lowering of TIFP. This notion is based on the present study that continuous i.v. administration of the vasodilating agent sodium nitroprusside lowered blood pressure by 20–25% but did not change TIFP over a 1 h study period. PGE_1 lowers IFP and leads to formation of edema in normal rat dermis, effects that most likely involve a decrease in the tension exerted by connective tissue cells on the ECM-

fiber network (31). Previously, we observed an increase in total tissue water in PROb tumors treated with PGE_1, suggesting that an interstitial edema was formed. The reduction in TIFP could thus cause an increased convection of fluid into the tumors and, in turn, the transport of soluble components such as 5-FU. Furthermore, an increase in fluid content in the interstitium will largely augment diffusion of compounds within the tissue (32). The effects of PGE_1 on 5-FU efficacy, therefore, could also be due to augmented distribution of 5-FU within the tumor tissue. Thus, an increased transcapillary fluid flux and subsequent increase of interstitial fluid volume would enhance both transport of 5-FU into the tumor and provide more favorable conditions for transport of fluid and solutes in the tumor interstitium.

Treatment with the effective combination of PGE_1 and 5-FU leads to an increase in apoptosis in the tumor viable zone. The possibility that PGE_1 had a direct effect on the PROb carcinoma cells, making them more sensitive to 5-FU, is less likely because no increase in apoptosis was observed when the two compounds were administered sufficiently separated in time. Similarly, expression of cytokeratin and the presence of more developed glandular structures were less pronounced in PROb tumors treated with the effective combination of PGE_1 and 5-FU. Based on the time dependence, that is, that 5-FU had to be injected during the time period of low TIFP for this effect to occur, it was most likely not due to PGE_1 increasing the sensitivity of PROb carcinoma cells to 5-FU. PGE_1 induces angiogenesis in the rabbit cornea and tumor disc angiogenesis models (33, 34). Our present results indicate that the potentiated efficacy of the combined PGE_1 and 5-FU treatment was not due to inhibition of angiogenesis or changes in tumor vasculature. The vessel density in the tumor viable zone was significantly decreased in tumors from all groups of animals receiving 5-FU. There was, however, no significant difference in vessel density between tumors that received 5-FU alone, or PGE_1 and 5-FU injected outside the time period when TIFP was low, compared with the tumors that had received the effective combination of PGE_1 and 5-FU, in spite of tumor growth retardation in the latter. It is therefore possible to conclude that the antitumor effect of the combination therapy was not due an antiangiogenetic mechanism.

We examined the possibility that tumor growth retardation in the syngeneic PROb model may be partly attributed to immunomodulatory effects of PGE_1. Analysis of the cellular composition of the tumor viable zone did not, however, reveal any significant differences in the density and distribution of T-lymphocytes, macrophages, or granulocytes in the tumors from any of the animal groups. The absence of MHC class II antigen expression in tumor tissues further strengthens the notion that the combination treatment did not induce an immune response in the tumors.

In summary, reduced TIFP enabled increased delivery and treatment efficiency of the low molecular weight cytostatic 5-FU in solid tumors. The potentiated effect of the treatment was observed on both tumor growth retardation and on changes in tumor morphology. The retardation of tumor growth was not due to immune responses or to changes in tumor vasculature. This concept is an important novel approach to effective anticancer drug delivery into solid tumors.

ACKNOWLEDGMENTS

This study was supported by grants from the Swedish Cancer Foundation (to K.R), the Norwegian Research Council (to R.K.R.), GustafV:s 80-årsfond (to K.R.), and BioPhausia AB. Ms. Ann-Marie Gustafson, Ms. Britta Isaksson, and Ms. Gerd Salvesen are gratefully acknowledged for technical assistance.

REFERENCES

1. Tannock, I. F. (1996) Treatment of cancer with radiation and drugs. *J. Clin. Oncol.* **14,** 3156–3174

2. Jain, R. K. (1998) The next frontier of molecular medicine: delivery of therapeutics. *Nat. Med.* **4,** 655–657

3. Yaun, I. (1998) Transvascular drug delivery in solid tumors. *Semin. Radiat. Oncol.* **8,** 164–175

4. Tannock, I. F. (2001) Tumor physiology and drug resistance. *Cancer Metastasis Rev.* **20,** 123–132

5. Vaupel, P., Kallinowski, F., and Okunieff, P. (1989) Blood flow, oxygen and nutrient supply, and metabolic microenvironment of human tumors: a review. *Cancer Res.* **49,** 6449–6465

6. Carmeliet, P., and Jain, R. K. (2000) Angiogenesis in cancer and other diseases. *Nature* **407,** 249–257

7. Netti, P. A., Berk, D. A., Swartz, M. A., Grodzinsky, A. J., and Jain, R. K. (2000) Role of extracellular matrix assembly in interstitial transport in solid tumors. *Cancer Res.* **60,** 2497–2503

8. Gullino, P., Clark, S., and Grantham, F. (1964) The interstitial fluid of solid tumors. *Cancer Res.* **24,** 780–797

9. Wiig, H., Tveit, E., R., H., Reed, R. K., and Weiss, L. (1982) Interstitial fluid pressure in DMBA-induced rat mammary tumours. *Scan. J. Clin. Lab. Invest.* **42,** 159–164

10. Philips, R., Bibby, M., and Double, J. (1990) A critical appraisal of the predictive value of an *in vivo* chemosensitivity assays. *J. Natl. Cancer Inst.* **82,** 1457–1469

11. Jain, R. K. (1987) Transport of molecules in tumor interstitium: a review. *Cancer Res.* **47,** 3039–3051

12. Leu, A. J., Berk, D. A., Lymboussaki, A., Alitalo, K., and Jain, R. K. (2000) Absence of functional lymphatics within a murine sarcoma: a molecular and functional evaluation. *Cancer Res.* **60,** 4324–4327

13. Griffon-Etienne, G., Boucher, Y., Brekken, C., Suit, H. D., and Jain, R. K. (1999) Taxane-induced apoptosis decompresses blood vessels and lowers interstitial fluid pressure in solid tumors: clinical implications. *Cancer Res.* **59,** 3776–3782

14. Rubin, K., Sjöquist, M., Gustafsson, A.-M., Isaksson, B., Salvesen, G., and Reed, R. K. (2000) Lowering of tumoral interstitial fluid pressure by prostaglandin E_1 is paralleled by an increased uptake of ^{51}Cr-EDTA. *Int. J. Cancer* **86,** 636–643

15. Emerich, D. F., Dean, R. L., Snodgrass, P., Lafreniere, D., Agostino, M., Wiens, T., Xiong, H., Hasler, B., Marsh, J., Pink, M., et al. (2001) Bradykinin modulation of tumor vasculature: II. activation of nitric oxide and phospholipase A2/prostaglandin signaling pathways synergistically modifies vascular physiology and morphology to enhance delivery of chemotherapeutic agents to tumors. *J. Pharmacol. Exp. Ther.* **296,** 632–641

16. Pietras, K., Östman, A., Sjöquist, M., Buchdunger, E., Reed, R. K., Heldin, C.-H., and Rubin, K. (2001) Inhibition of platelet-derived growth factor receptors reduces interstitial hypertension and increases transcapillary transport in tumors. *Cancer Res.* **61,** 2929–2034

17. Pietras, K., Rubin, K., Sjöblom, T., Buchdunger, E., Sjöquist, M., Heldin, C.-H., and Östman, A. (2002) Inhibition of PDGF receptor signaling in tumor stroma enhances antitumor effect of chemotherapy. *Cancer Res.* **62,** 5476–5484

18. Sirotnak, F. M., Zakowski, M. F., Miller, V. A., Scher, H. I., and Kris, M. G. (2000) Efficacy of cytotoxic agents against human tumor xenografts is markedly enhanced by coadministration of ZD1839 (Iressa), an inhibitor of EGFR tyrosine kinase. *Clin. Cancer Res.* **6,** 4885–4892

19. Fisher, G. A., Cho, C. D., Halsey, J. Z., Advani, R. H., Yuen, A. R., Lum, B. L., and Sikic, B. I. (2002) A phase I study of ZD 1839 (Iressa) in combination with oxaliplatin, 5-fluorouracil (5-FU) and leucovorin (LV) in advanced solid malignancies. *Eur. J. Cancer* **38,** 63

20. Trifan, O. C., Durham, W. F., Salazar, V. S., Horton, J., Levine, B. D., Zweifel, B. S., Davis, T. W., and Masferrer, J. L. (2002) Cyclooxygenase-2 inhibition with celecoxib enhances antitumor efficacy and reduces diarrhea side effect of CPT-11. *Cancer Res.* **62,** 5778–5784

21. Bagnato, A., Cirilli, A., Salani, D., Simeone, P., Muller, A., Nicotra, M. R., Natali, P. G., and Venuti, A. (2002) Growth inhibition of cervix carcinoma cells in vivo by endothelin A receptor blockade. *Cancer Res.* **62,** 6381–6384

22. Lau, C., Mole, M. L., Copeland, M. F., Rogers, J. M., Kavlock, R. J., Shuey, D. L., Cameron, A. M., Ellis, D. H., Logsdon, T. R., Merriman, J., et al. (2001) Toward a biologically based dose-response model for developmental toxicity of 5-fluorouracil in the rat: acquisition of experimental data. *Toxicol. Sci.* **59,** 37–48

23. Martin, M., Åhlen, K., Dimanche-Boitrel, M. T., Mendrick, D. L., Turner, D. C., Rubin, K., and Martin, F. (1996) Colon-cancer cell variants producing regressive tumors in syngeneic

rats, unlike variants yielding progressive tumors, attach to interstitial collagens through integrin α2β1. *Int. J. Cancer* **65,** 796–804

24. Kellar, K. E., Fujii, D. K., Gunther, W. H., Briley-Saebo, K., Björnerud, A., Spiller, M., and Koenig, S. H. (2000) NC100150 Injection, a preparation of optimized iron oxide nanoparticles for positive-contrast MR angiography. *J. Magn. Reson. Imaging* **11,** 488–494

25. Turetschek, K., Huber, S., Floyd, E., Helbich, T., Roberts, T. P., Shames, D. M., Tarlo, K. S., Wendland, M. F., and Brasch, R. C. (2001) MR imaging characterization of microvessels in experimental breast tumors by using a particulate contrast agent with histopathologic correlation. *Radiology* **218,** 562–569

26. Björnerud, A., Johansson, L. O., Briley-Saebo, K., and Ahlström, H. K. (2002) Assessment of T1 and T2* effects in vivo and ex vivo using iron oxide nanoparticles in steady state–dependence on blood volume and water exchange. *Magn. Reson. Med.* **47,** 461–471

27. Sundberg, C., Ivarsson, M., Gerdin, B., and Rubin, K. (1996) Pericytes as collagen-producing cells in excessive dermal scarring. *Lab. Invest.* **74,** 452–466

28. Gundersen, H. J., Bendtsen, T. F., Korbo, L., Marcussen, N., Möller, A., Nielsen, K., Nyengaard, J. R., Pakkenberg, B., Sörensen, F. B., Vesterby, A., et al. (1988) Some new, simple and efficient stereological methods and their use in pathological research and diagnosis. *APMIS* **96,** 379–394

29. Wassberg, E., Hedborg, F., Sköldenberg, E., Stridsberg, M., and Christofferson, R. (1999) Inhibition of angiogenesis induces chromaffin differentiation and apoptosis in neuroblastoma. *Am. J. Pathol.* **154,** 395–403

30. Emerich, D. F., Snodgrass, P., Dean, R. L., Lafreniere, D., Agostino, M., Wiens, T., Xiong, H., Hasler, B., Marsh, J., Pink, M., et al. (2001) Bradykinin modulation of tumor vasculature: I. Activation of B2 receptors increases delivery of chemotherapeutic agents into solid peripheral tumors, enhancing their efficacy. *J. Pharmacol. Exp. Ther.* **296,** 623–631

31. Berg, A., Ekwall, A. K., Rubin, K., Stjernschantz, J., and Reed, R. K. (1998) Effect of PGE_1, PGI_2, and $PGF_{2\alpha}$ analogs on collagen gel compaction *in vitro* and interstitial pressure *in vivo*. *Am. J. Physiol.* **274,** H663–H671

32. Aukland, K., and Reed, R. K. (1993) Interstitial-lymphatic mechanisms in the control of extracellular fluid volume. *Physiol. Rev.* **73,** 1–78

33. Gullino, P. M. (1995) Prostaglandins and gangliosides of tumor microenvironment: their role in angiogenesis. *Acta Oncol.* **34,** 439–441

34. Nelson, M. J., Conley, F. K., and Fajardo, L. F. (1993) Application of the disc angiogenesis system to tumor-induced neovascularization. *Exp. Mol. Pathol.* **58,** 105–113

Received January 24, 2003; accepted May 22, 2003.

Table 1

Quantification of vascularization in PROb tumor tissues[a]

Definition	5-FU 15 min before PGE_1 (n=4)	5-FU 1 min after PGE_1 (n=4)	PBS and 5-FU (n=4)	PGE_1 and PBS (n=4)
CD31-positive structures (density per mm^2 in the tumor viable zone)	101 ± 17	84 ± 14	92 ± 21	158 ± 17*
Fraction of viable grids (%)	42	45	54	54
Length of vessels per tumor volume (length density, mm^{-2})	24 ± 2	22 ± 4	22 ± 6	35 ± 5*
Volume of vessels per tumor volume (volumetric density)	0.11 ± 0.02	0.14 ± 0.03	0.11 ± 0.03	0.19 ± 0.05**
Surface area of vessels per tumor volume (surface density, mm^{-1})	3.7 ± 0.4	3.4 ± 0.4	3.2 ± 0.8	5 ± 1*
Mean section area of vessels ($10^{-3} \times mm^2$)	4.65 ± 1.04	6.4 ± 0.6***	5.0 ± 0.7	5.4 ± 0.7
Mean boundary length of vessels (mm)	0.14 ± 0.01	0.16 ± 0.01[#]	0.14 ± 0.02	0.14 ± 0.02
Mean diameter of vessels (mm)	0.076 ± 0.007	0.089 ± 0.004***	0.079 ± 0.006	0.082 ± 0.005

[a]Tumor tissue sections were analyzed (20–82 fields of vision, ×500) using a stereometric approach. The density of CD31-positive structures per mm^2 was counted in the tumor viable zone (20 random fields of vision, ×200). Significant difference: *between the animal group receiving PGE_1 and PBS compared with all groups receiving 5-FU; **between the animal group receiving PGE_1 and PBS compared with groups receiving PBS and 5-FU, or 5-FU 15 min before PGE_1; ***between the group receiving 5-FU 1 min after PGE_1 compared with the groups receiving 5-FU 15 min before PGE_1 or PBS and 5-FU; [#]between the group receiving 5-FU 1 min after PGE_1 compared with the group receiving 5-FU 15 min before PGE_1. $P<0.05$.

Fig. 1

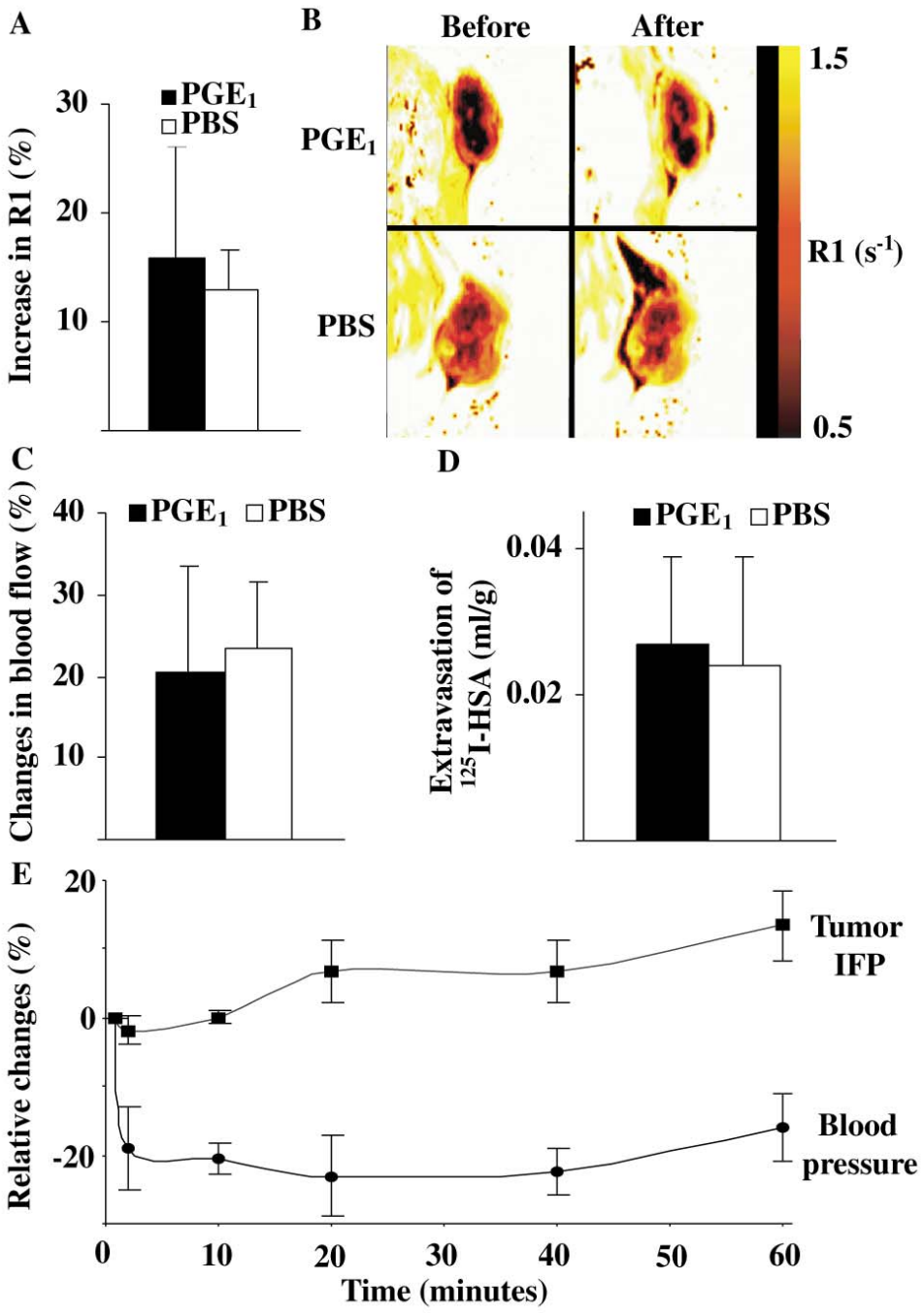

Figure 1. Vascular hemodynamic effects of PGE_1 treatment in PROb tumors. A) Effects of PGE_1 on tumor blood volume were determined by MR imaging and expressed as changes in R1 (see Material and Methods). There was no significant increase in PROb tumor blood volume after treatment with PGE_1 compared with PBS. **B)** R1 maps of PROb tumors from two animals, one treated with PGE_1 and one with PBS, before and after injection of the intravascular contrast agent, NC100150. The enhancement pattern is similar in both animals. **C)** Blood flow in PROb tumors. Blood flow was determined using microspheres labeled with two different radioactive isotopes. They were injected before and 15 min after the instillments of PGE_1 or PBS. The increase in blood flow is not significantly different in animals that received PGE_1 compared with PBS. **D)** Extravasation of radioactive human albumin. Instillment of PGE_1 did not significantly increase albumin extravasation compared with instillment of PBS. **E)** Effect of lowering blood pressure on TIFP. Lowering of blood pressure by continuous i.v. infusion of sodium nitroprusside did not affect the TIFP in PROb carcinomas.

Fig. 2

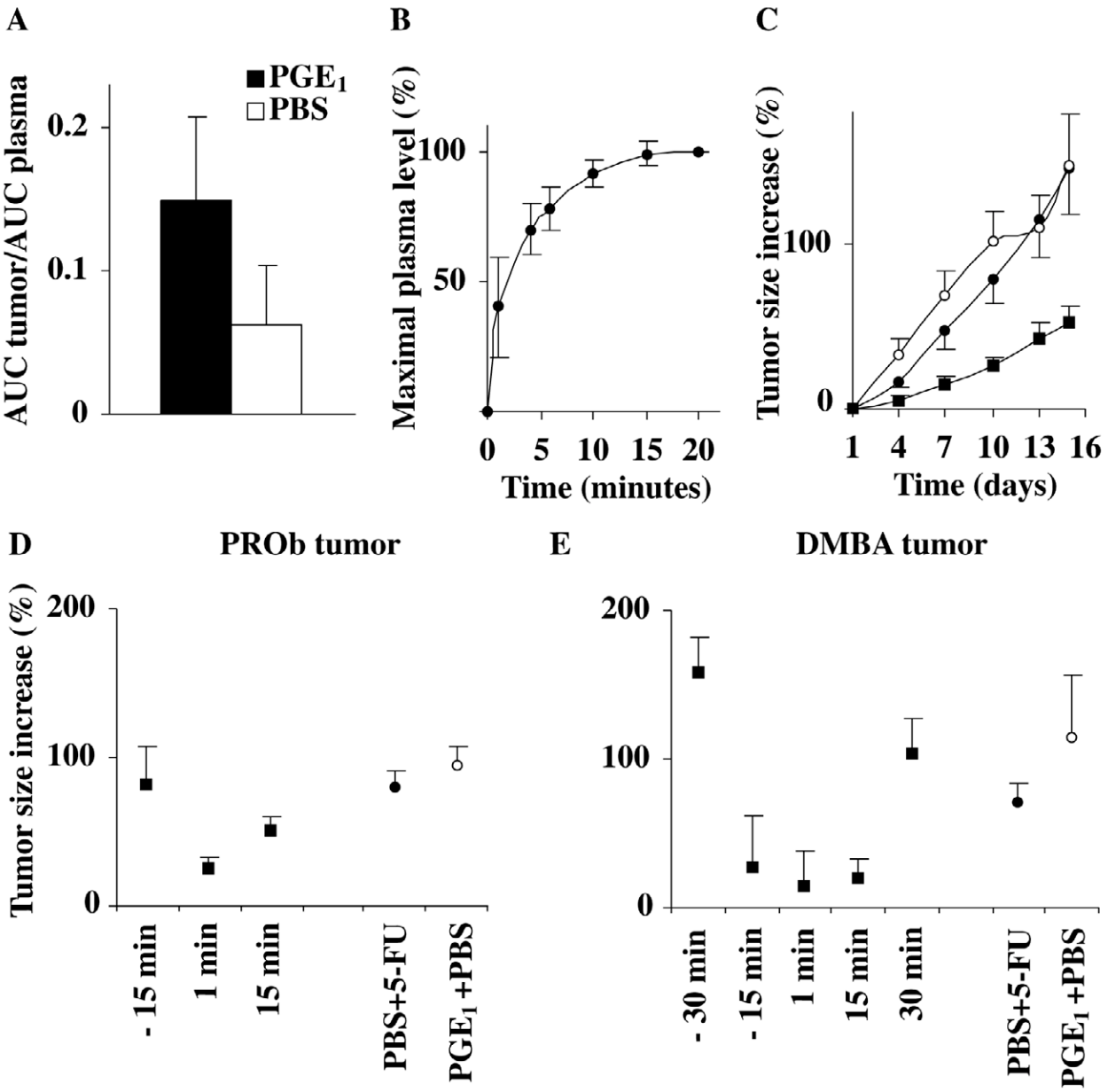

Figure 2. Time dependence of the synergism between 5-FU and PGE_1. A) PGE_1 increases the transcapillary transport of 5-FU into the tumor interstitium. Microdialysis of [^{3}H]5-FU was performed on rats bearing PROb tumors. AUC were measured during the first 30 min after i.v. injection. Longer periods of measurements were avoided due to the rapid metabolism of 5-FU. PGE_1 (*n*=6) or PBS (*n*=6) was injected s.c. around the tumor simultaneously with the i.v. injection of [^{3}H]5-FU. After injection of PGE_1, the ratio between [^{3}H]5-FU level in plasma and in the tumor was significantly increased compared with animals receiving a PBS injection. **B)** Dynamics of [^{3}H]5-FU accumulation in blood following i.p. injection. [^{3}H]5-FU (37 MBq) was administered i.p. into BD-IX rats (*n*=4), and blood samples (20 µl) were collected at different time points during a 20-min period. **C)** Growth rate of PROb tumors. Sizes were measured externally every third day during the treatment period. Data are presented as a percentage of tumor size increase with the sizes at day 1 set to 100%. Filled squares, PGE_1 followed 1 min later by 5-FU (*n*=11); open circles, PGE_1 followed by PBS (*n*=5); and filled circles, PBS followed by 5-FU (*n*=11). At all time points after day 3, the tumor size increase in the group receiving PGE_1 followed 1 min later by 5-FU was significantly lower ($P<0.05$) than the two control groups. **D**, **E)** Size increase of PROb- and DMBA-induced tumors at day 10 of the experiment (Mean ±SE). 5-FU was administered i.p. at various time points before PGE_1 instillment (designated by –) or after PGE_1 instillment.

Fig. 3

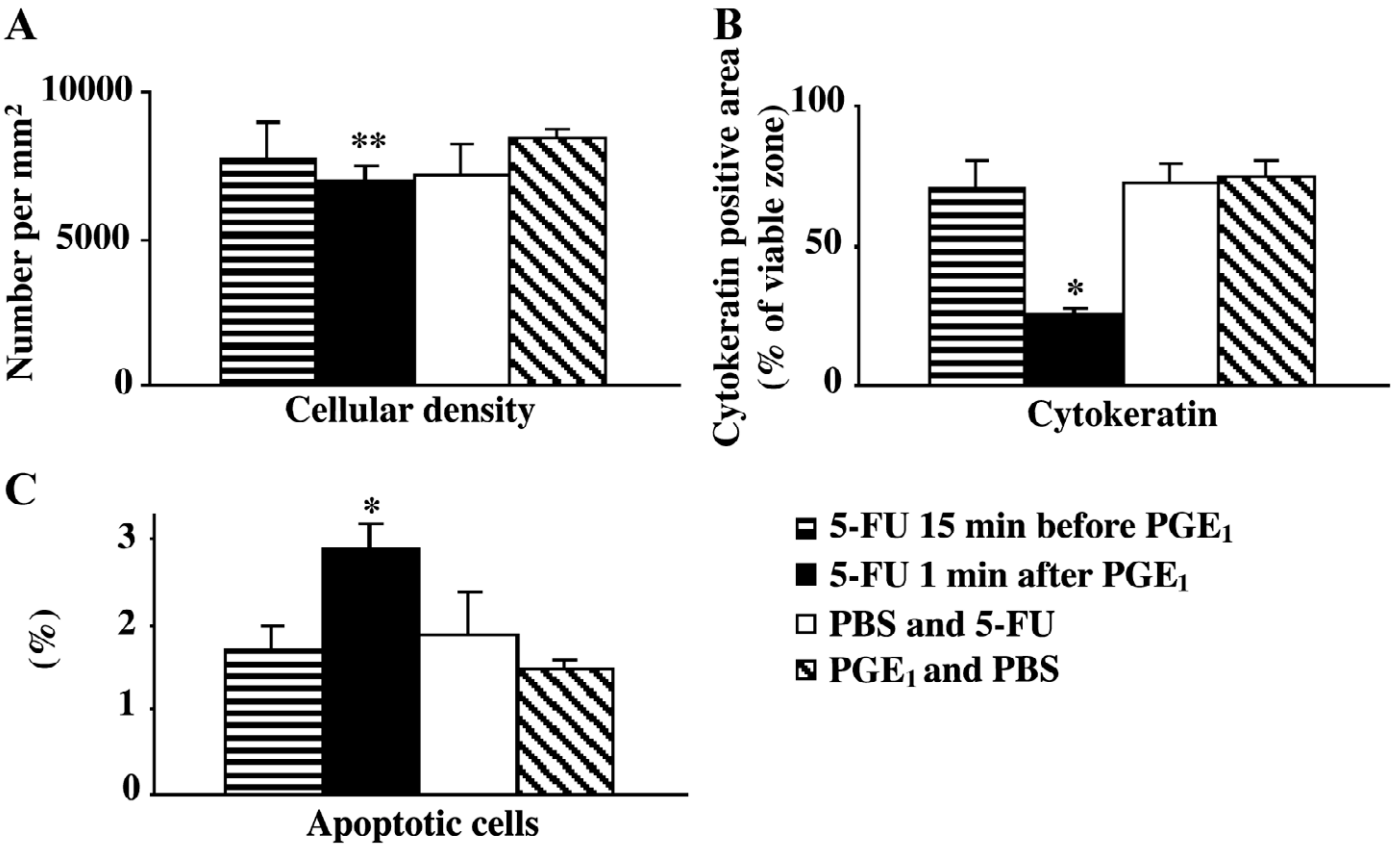

Figure 3. Effects on cellular density, cytokeratin expression, and apoptosis in PROb tumors treated with the combination of 5-FU and PGE_1. Tissue sections (3–9 per group) were analyzed (15–24 random fields of vision, ×500), and cellular density and apoptotic cells were manually counted using a counting grid. The area occupied by tumor cells expressing cytokeratins was calculated using image analysis software. The apoptotic index was calculated as the percentage of immunoreactive nuclei divided by the total number of cell nuclei counted. *Significant difference between the animal group receiving 5-FU 1 min after PGE_1 instillment compared with the other three groups. **Significant difference between the animal group receiving 5-FU 1 min after PGE_1 instillment compared with the group receiving PGE_1 and PBS. $P<0.05$.

Fig. 4

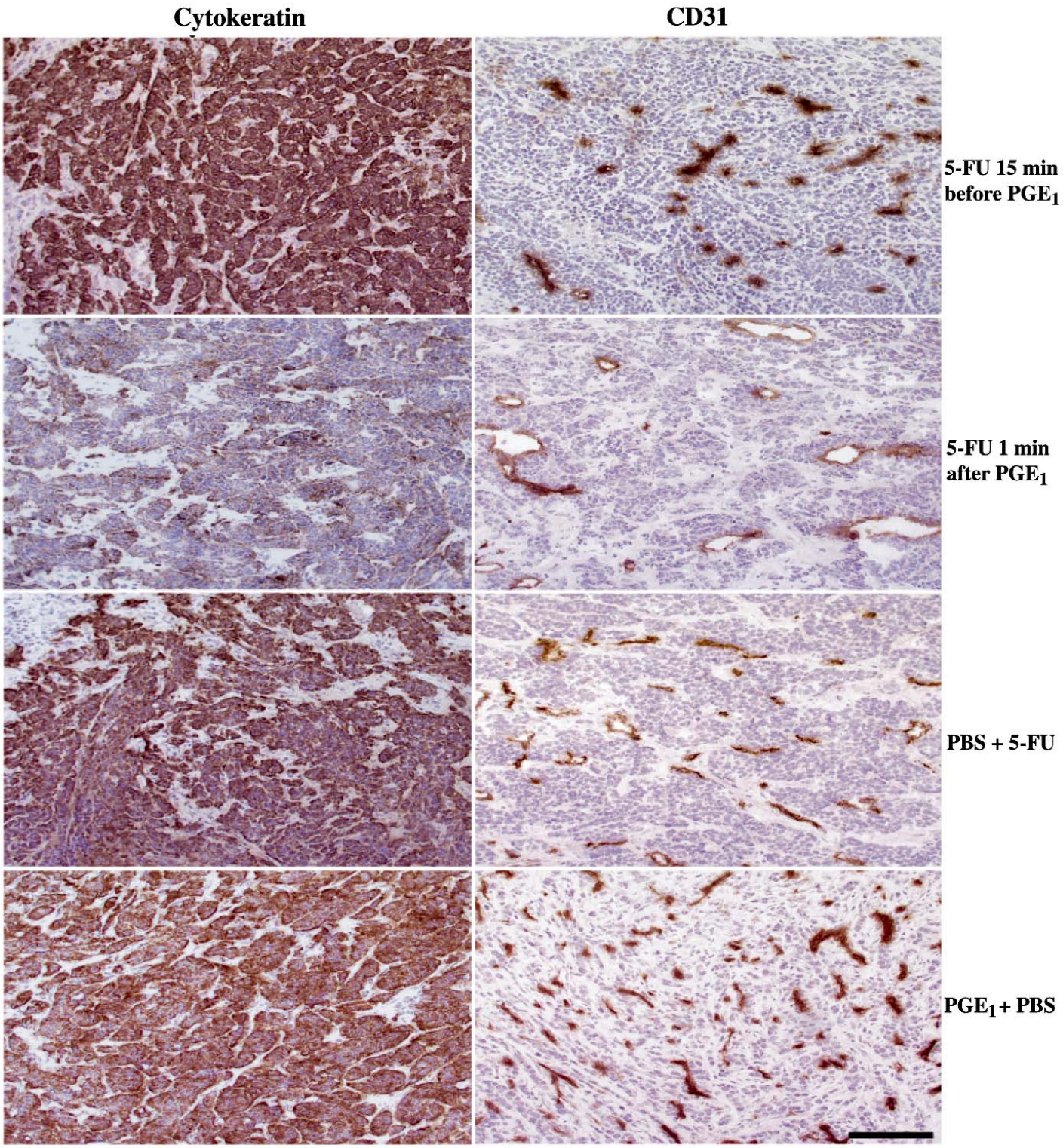

Figure 4. Effects on PROb tumor morphology by combination treatment with 5-FU and PGE_1. Immunohistochemistry using an anti-pan cytokeratin and CD31/PECAM-1 antibody was performed. A significant decrease in cytokeratin expression in the tumors from animals receiving 5-FU 1 min after PGE_1 instillment was observed. Vascular parameters were also changed in this group. *Bar*, 100 μm.

Fig. 5

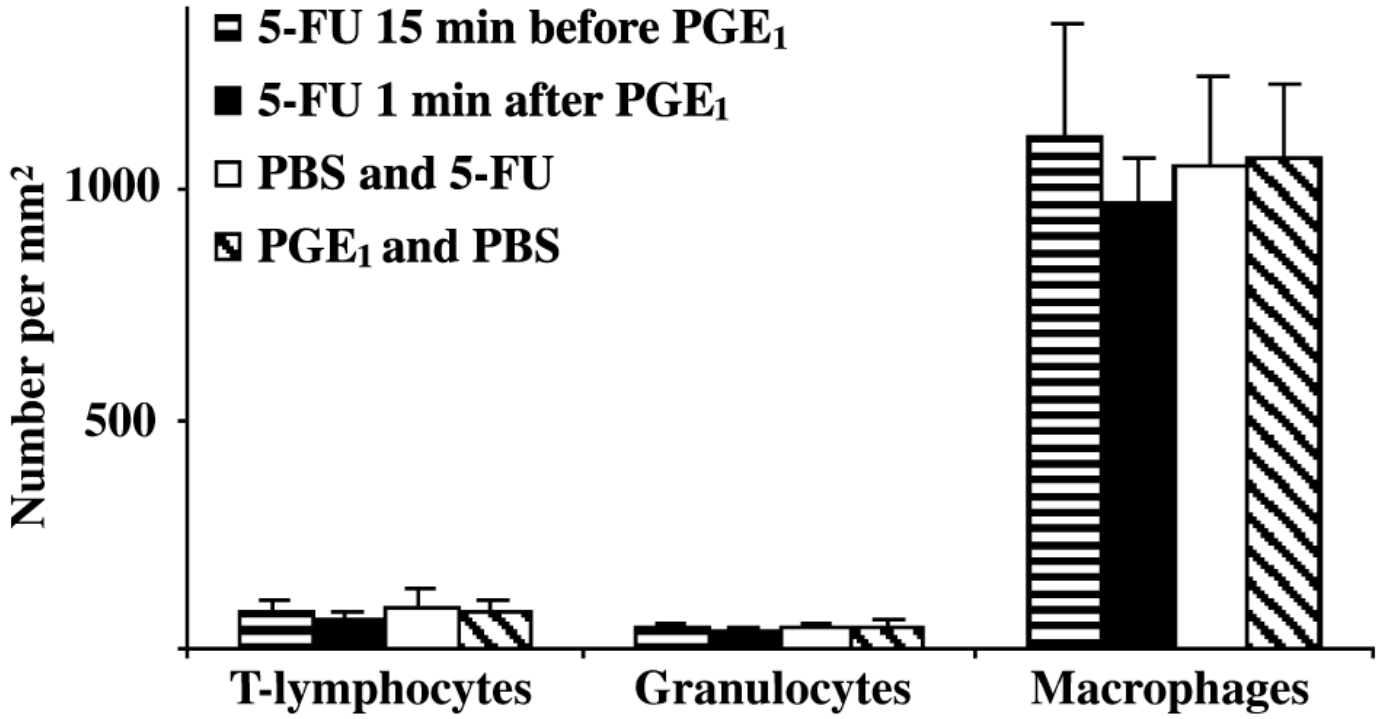

Figure 5. Leukocyte infiltration in the viable zone of PROb tumors treated with the combination of 5-FU and PGE_1. Sections (4-9 per group) were analyzed (15-24 random fields of vision, x500) and cells were manually counted using a counting grid.